

*Supporting Information
of*

**Rational Design of Metal-Ligands for Conversion of CH₄ and CO₂ to Acetates:
Role of Acids and Lewis acids**

Bangaru Bhaskararao,* Dong Yeon Kim, Jenica Marie L. Madridejos, Cheol-Min Park and Kwang S. Kim*

Department of Chemistry, Ulsan National Institute of Science and Technology (UNIST), Ulsan 44919, Korea

*Corresponding authors: kimks@unist.ac.kr (ksk) or bangaru.bhaskararao@gmail.com (bb)

Sr. No	Table of Contents	Page Number
1	Quasi Treatment for Gibbs Free Energies	3
2	Gibbs Free Energy Barriers for Diverse Noyori-type Catalysts	4
3	Tunneling Corrections	5
4	Role of Acids for CH ₄ Activation	6
5	Role of Lewis Acids for CO ₂ Activation	7
6	Mechanism, Energy profile and Transition states using Ru-OO	8
7	Mechanism, Energy profile and Transition states using Ru-PP	10
8	Effects of Pressure and Temperature	11
9	Mechanism, Energy profile and Transition states using Rh/Ir-PP	12
10	Effect in Gas vs Solvent Phase Optimization	14
11	CO ₂ activation using 2 molecules of AlCl ₃	15
12	Effect of Basis sets and Quasi Approximation on Energy Profiles	17
13	Effects of Substitution on Ligands	18
14	Comparison of CO ₂ Activations for sp ³ (CH ₄) versus sp ² (C ₆ H ₆)	19
15	NBO Analysis of CH ₄ and CO ₂ activation steps	20

1. Quasi Treatment for Gibbs Free Energies

Gibbs free energies (ΔG) for the $\text{CH}_4 + \text{CO}_2 = \text{CH}_3\text{COOH}$ reaction are also obtained by using the quasi-harmonic entropic approximation (QHA) based on the Grimme and Truhlar method^[1] (the frequency cut-off was 100 cm^{-1}). We note that a half of QHA correction (QHA/2) is more realistic using M06/6-31G** [expt: 13.2 kcal/mol in water, versus DFT(L2+QHA/2): 14.2 kcal/mol in benzene; Table S1]. M06/def2TZVP overestimates the Gibbs free energies for this particular system. Table S10 also shows 50% quasi treatment of relative Gibbs free energy profiles in benzene solvent.

CH ₄ + CO ₂ = CH ₃ COOH									
	Experimental		DFT Calculations						
	gas	liquid	L1	L2	L2+QHA	L2+QHA/2	L3	L4	L4+QHA
ΔG	16.98	13.18	20.3	16.6	11.7	14.2	25.2	21.4	16.3

L1 = [M06/6-31G**]

L2 = [SMD_(benzene)]/[M06/6-31G**]

L3 = [M06/def2TZVP]

L4 = [SMD_(benzene)]/[M06/def2TZVP]

QHA/2: 50% QHA correction

Table S1. Relative Gibbs free energies (from the separated reactants) of [1-2] \ddagger and [3-4] \ddagger using various metal complexes with different ligands calculated at the SMD_(benzene)/M06/(6-31G**,SDD) level. The low-freq-corrections (100 cm^{-1}) in ΔG values are given.

Complexes	$\Delta G_{\text{benzene}}^{298K}$		low-freq corrected $\Delta G_{\text{benzene}}^{298K}$		Difference in ΔG between without and with low-freq-correction for [1-2] \ddagger & [3-4] \ddagger
	[1-2] \ddagger	[3-4] \ddagger	[1-2] \ddagger	[3-4] \ddagger	
Ru-OO	35.6	49.4	30.5	39.6	5.1 & 9.8
Ru-NNTs	38.6	47.6	33.8	38.1	4.8 & 9.5
Ru-PP	22.1	41.6	16.8	31.6	5.3 & 10.0

2. Gibbs Free Energy Barriers for Diverse Noyori-type Catalysts

Table S2. Gibbs free energies barriers (in kcal/mol; **TS1** and **TS2** with respect to the separated reactants = 0.0 kcal/mol) for various metal complexes with diverse ligands at the M06/(6-31G**,SDD) level of theory.

Complexes	ΔG_{gas}^{298K}	
	[1-2] [‡]	[3-4] [‡]
Ru(C ₆ H ₆)(O,O)	34.7	50.2
Ru(C ₆ H ₆)(N,NTs)	40.2	48.3
Ru(C ₆ H ₆)(N,N)	41.7	48.8
Ru(C ₆ H ₆)(N,O)	41.1	58.1
Ru(C ₆ H ₆)(S,S)	44.7	75.5
Rh-(C ₅ H ₅)(O,O)	35.0	49.4
Ir-(C ₅ H ₅)(O,O)	40.9	55.9
Ru-(C ₅ H ₅)(P,P)	20.4	43.2
Rh-(C ₅ H ₅)(P,P)	21.3	46.1
Ir-(C ₅ H ₅)(P,P)	28.2	57.2

3. Tunneling Corrections

The Imaginary frequencies of CH₄ and CO₂ activation transition states are

TS[1-2] ($\nu = -1501.6 \text{ cm}^{-1}$ or 4.29 kcal/mol): the tunneling driven effective activation barrier lowering (ΔE) is -1.42 kcal/mol .

TS[3-4] ($\nu = -367.5 \text{ cm}^{-1}$ or 1.05 kcal/mol): the tunneling driven effective activation barrier lowering (ΔE) is -0.06 kcal/mol .

According to Wigner,^[2] the effect of tunneling correction is

$$\frac{k_{\text{quantum}}(T)}{k_{\text{classical}}(T)} = 1 + \frac{1}{24} \left(\frac{\hbar\nu}{k_B T} \right)^2 = 1 + \frac{1}{24} u^2,$$

where \hbar is the Planck constant, $\nu_{TS} = i \nu$ is the imaginary frequency ($\nu > 0$), k_B is the Boltzmann constant, T is the absolute temperature, and $u = \hbar\nu/k_B T$. This equation holds only for small u . If u is a little larger, then Bell's tunneling correction^[3] is used. The tunneling driven effective activation barrier lowering (ΔE) is

$$\frac{\Delta E}{kT} = \frac{u}{2} \cot\left(\frac{u}{2}\right) - 1$$

4. Role of Acids for CH₄ Activation

Table S3. Relative Gibbs free energy barriers of C-H activation of CH₄ in the presence and absence of acid additives of Ru/Rh/Ir metal complexes with NNTs/OO/PP ligands.

C-H activation		M-NNTs			M-OO			M-PP		
Acid	pKa	Ru	Rh	Ir	Ru	Rh	Ir	Ru	Rh	Ir
----	----	40.2	37.4	43.7	34.7	35.0	40.9	20.4	21.4	28.1
(CH ₃) ₃ COOH	(5.03)	30.0	--	--	35.9	--	--	--	--	--
CH ₃ COOH	(4.74)	27.3	44.4	45.4	34.5	38.5	40.0	43.8	--	--
CCl ₃ COOH	(0.64)	33.1	--	--	43.8	--	--	32.9	--	--
CF ₃ COOH	(0.23)	30.9	42.3	42.6	28.6	40.1	33.4	52.2	--	--
		concerted metalation deprotonation			concerted metalation deprotonation			concerted “oxidative addition-reductive elimination”		
		8-membered TS ($\nu = i 1637.6 \text{ cm}^{-1}$)			8-membered TS ($\nu = i 1449.6 \text{ cm}^{-1}$)			4-membered TS ($\nu = i 530.9 \text{ cm}^{-1}$)		

5. Role of Lewis Acids for CO₂ Activation

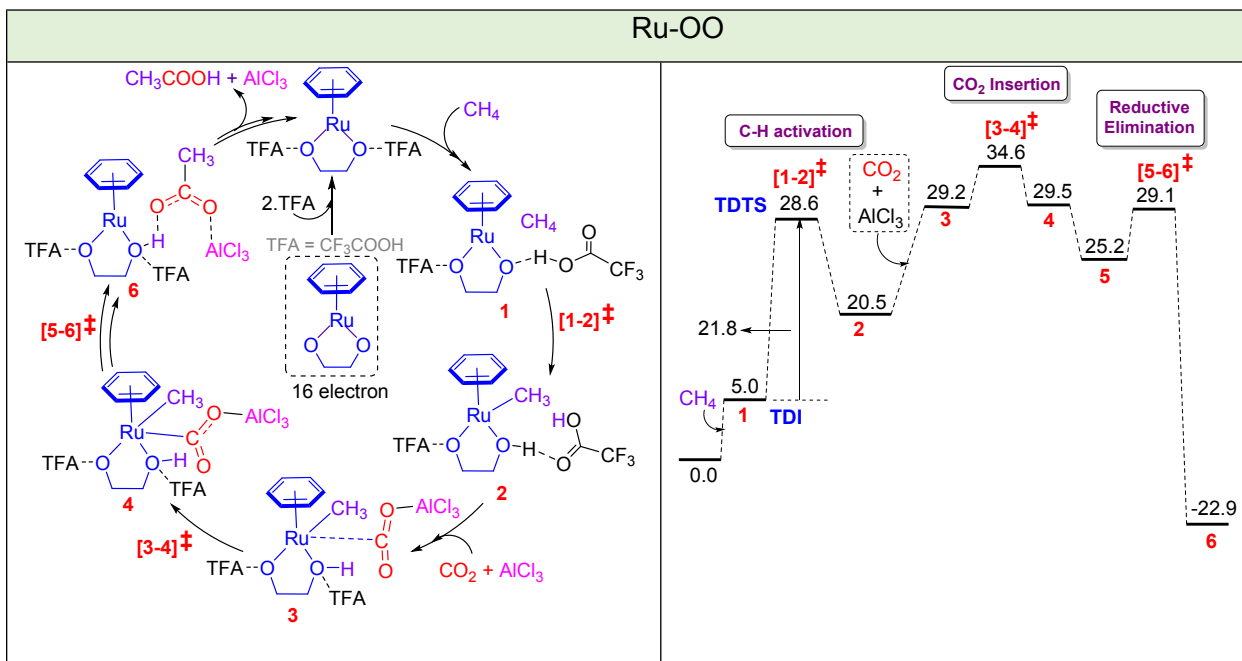
Table S4. Relative Gibbs free energies of C-C bond formation between CH₄ and CO₂...LA(Lewis Acid) ([5-6]‡) using different metal based Lewis acids with Ru-PP complex.

	Lewis Acids	Ru-PP
1	AlCl ₃	9.8
2	LiCl	19.6
3	LiClO ₄	23.6
4	ZnCl ₂	27.9
5	Al(Me) ₃	34.6
6	TiCl ₄	36.8
7	BPh ₃	47.9
8	SiCl ₄	55.5
9	Me ₃ SiCl	57.2

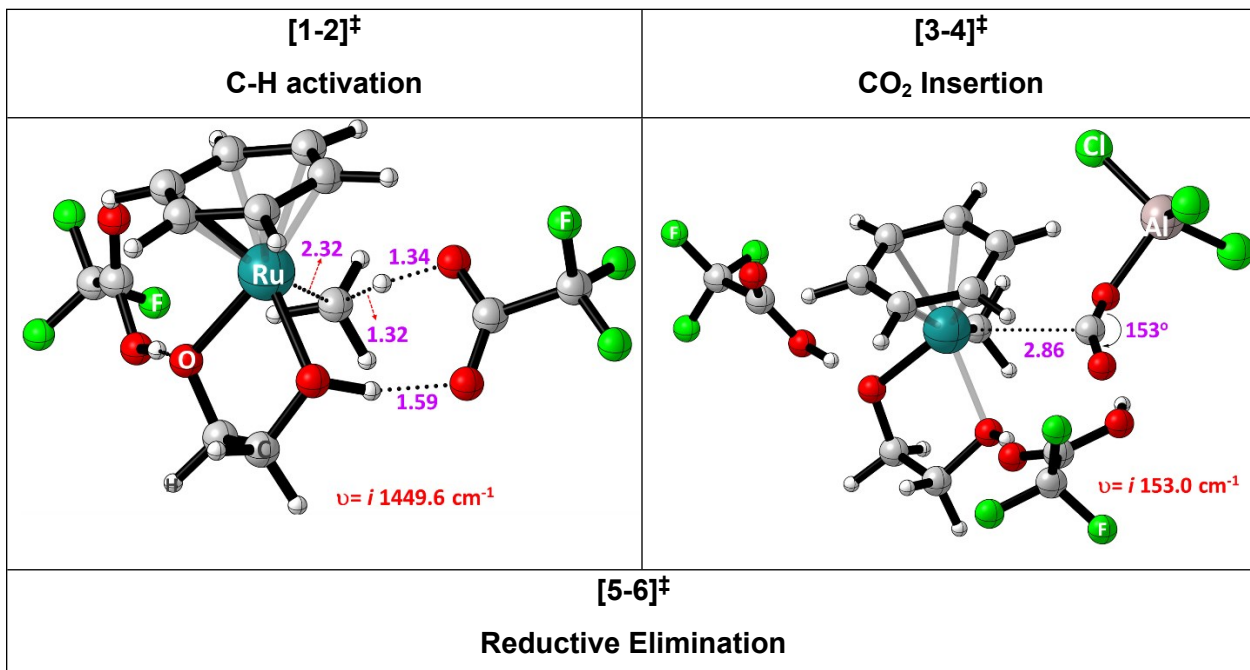
Table S5. Relative Gibbs free energies of CO₂ activation using different metal based Lewis acids with Ru-PP/NNTs-AA/OO-2TFA complexes calculated at M06/(6-31G**,SDD) level of theory.

Lewis Acids	Ru-NNTs.AA		Ru-AA.OO-2TFA		Ru-PP	
	[3-4]‡	[5-6]‡	[3-4]‡	[5-6]‡	[3-4]‡	[5-6]‡
--	48.3		50.2		46.4	
AlCl ₃	23.3	17.2	34.6	29.1	8.4	9.8
LiCl	--	19.7	--	33.7	--	19.6
LiClO ₄	--	27.5	--	36.5	--	23.6

6. Mechanism, Gibbs Free Energy Profile and Transition states using Ru-OO



Scheme S1. Detailed mechanism and corresponding Gibbs free energy profile calculated at the M06/(6-31G**,SDD) level for the formation of acetate/acetic acid from CH_4 and CO_2 using Ru-OO complex in the presence of co-catalysts (trifluoroacetic acid-TFA and Lewis acid- AlCl_3).



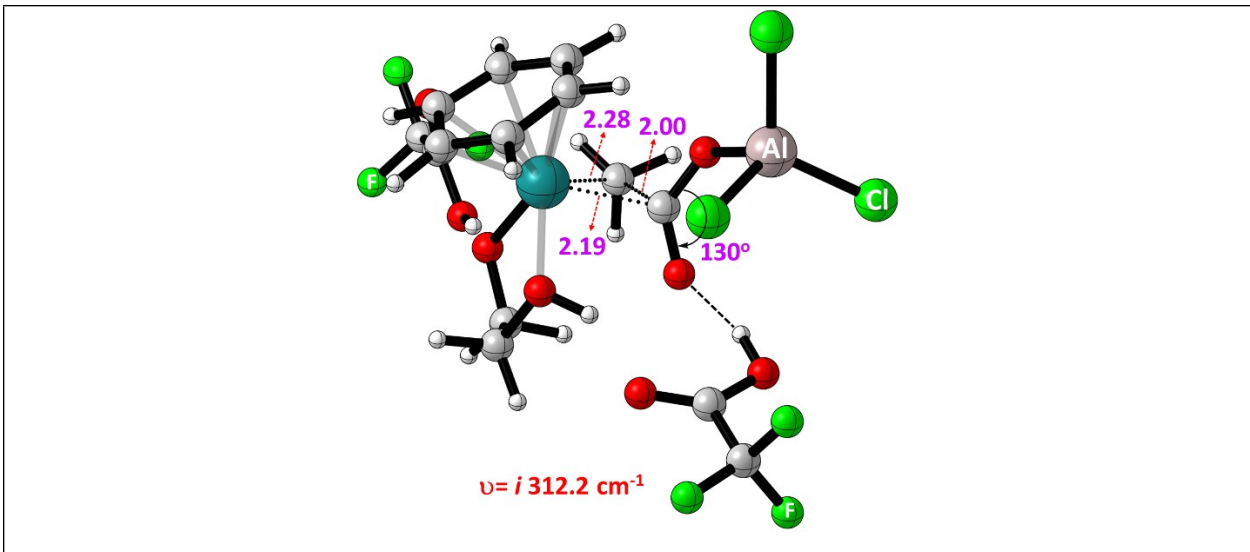


Figure S1. Optimized geometries of the transition states of carboxylation of CH_4 with CO_2 using Ru- $\text{OO}\square\text{2TFA}$ complexes in the presence of Lewis acid AlCl_3 . All distances are in angstroms.

Table S6. Relative Gibbs free energy profile of the formation of acetates using Ru- $\text{OO}.2\text{TFA}$ complex in the presence of Lewis acid and effect of quasi approximation (50% quasi treatment) also shown here.

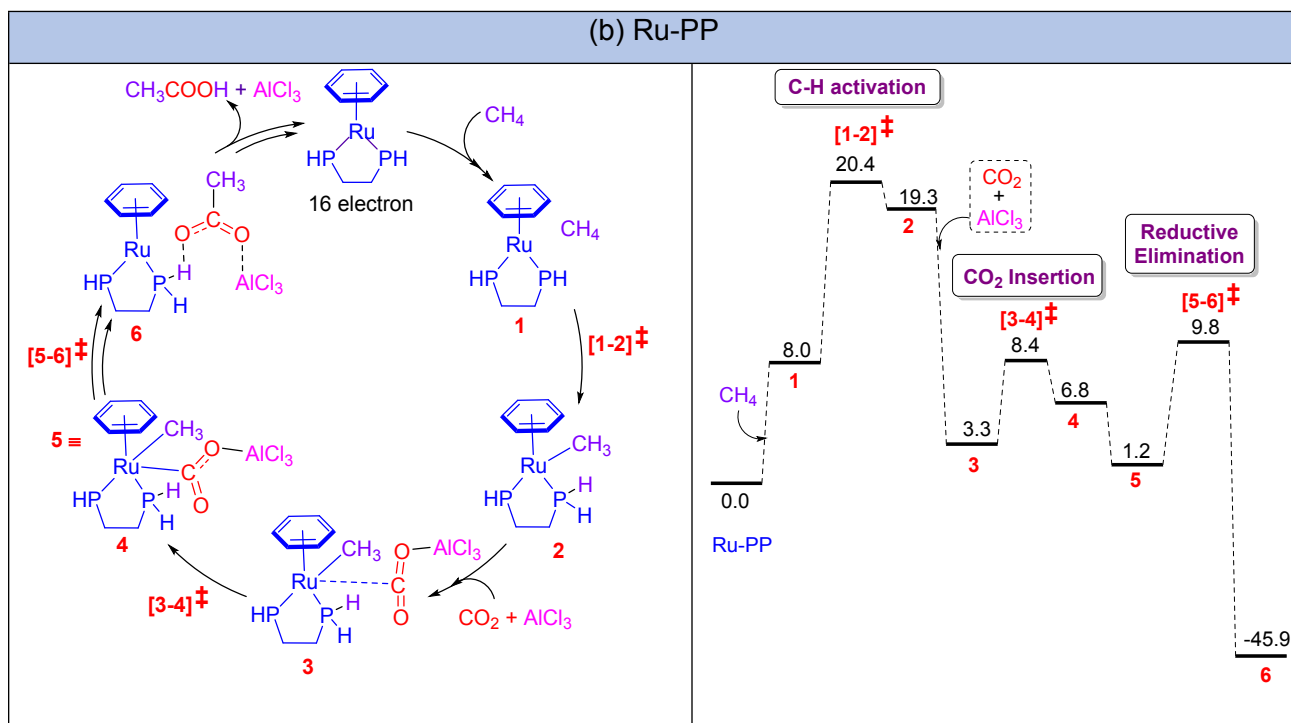
Ru- $\text{OO}\square\text{2TFA}$				
	L1	L2□	L4□	L4□ + QHA/2
1	5.0	5.8	5.7	4.5
[1-2]‡	28.6	27.4	27.7	25.8
2	20.5	18.8	19.8	17.6
3	29.2	28.5	30.2	23.3
[3-4]‡	34.6	36.2	36.0	28.9
4	29.5	26.5	28.3	22.2
5	25.2	21.6	23.5	17.5
[5-6]‡	29.1	25.4	27.3	21.4
6	-22.9	-24.2	-23.3	-30.3

L1=M06/[6-31G**, SDD(Ru)]

L2□ =[SMD_(DCM)/M06/6-31G**, SDD(Ru)]/[M06/6-31G**, SDD(Ru)]

L4□: [SMD_(benzene)/M06/6-31G**, SDD(Ru)]/[M06/6-31G**, SDD(Ru)]

7. Mechanism, Gibbs Free Energy Profile and Transition states using Ru-PP



Scheme S2. Detailed mechanism and corresponding Gibbs free energy profile calculated at M06/(6-31G^{**},SDD) for the formation of acetate/acetic acid from CH_4 and CO_2 using Ru-PP in the presence of Lewis acid- AlCl_3 .

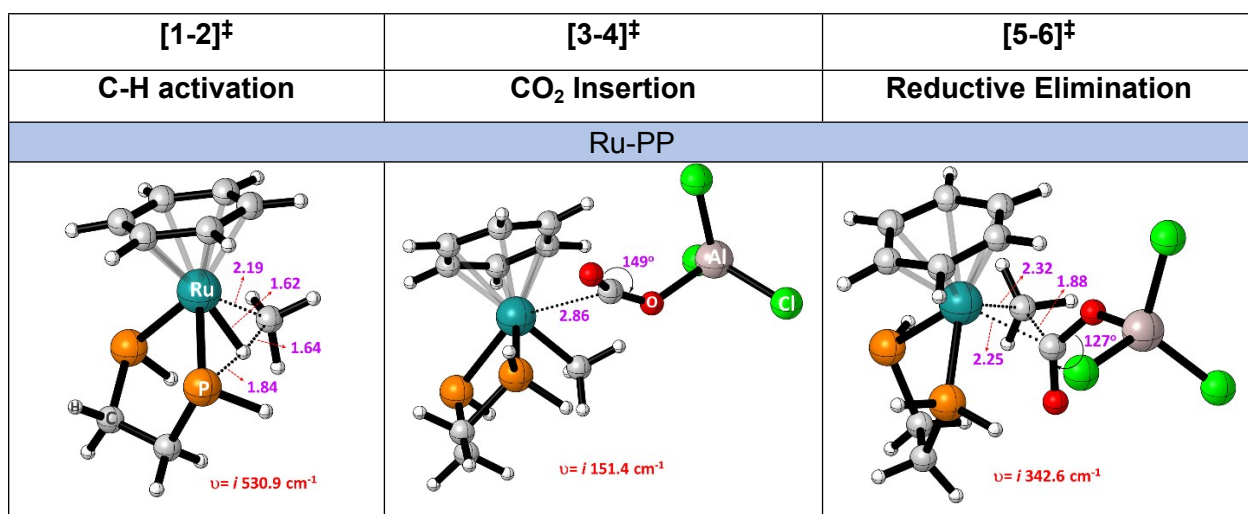


Figure S2. Optimized geometries of the transition states of carboxylation of CH₄ with CO₂ using Ru-PP complex (Scheme S2) in the presence of Lewis acid AlCl₃. All distances are in angstroms.

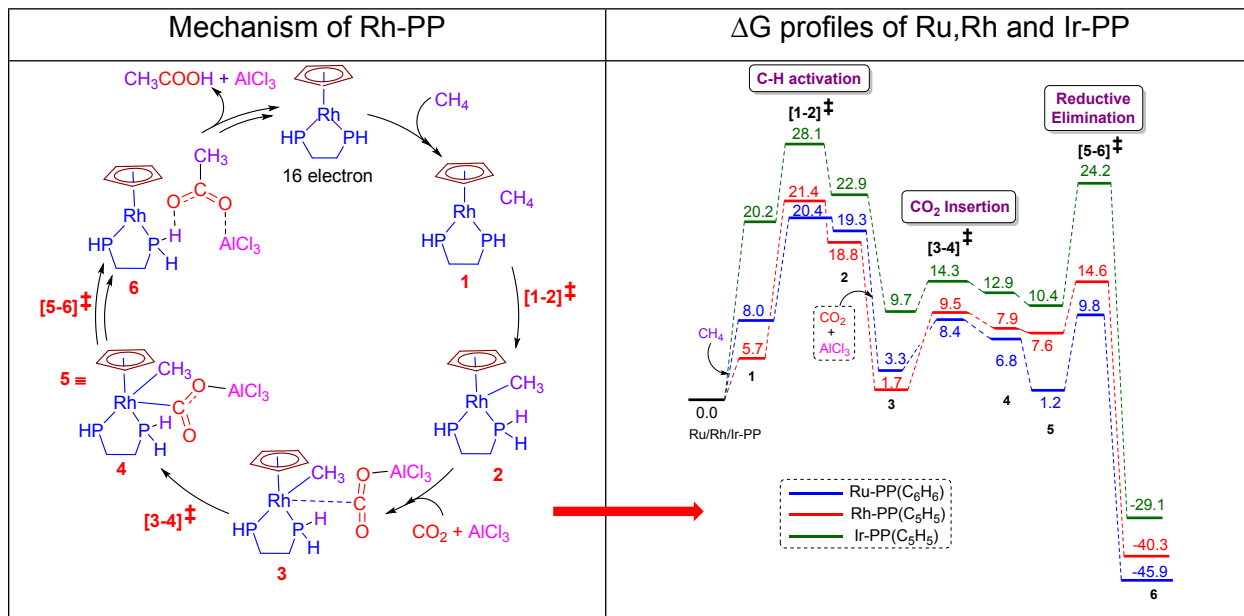
8. Effects of Pressure and Temperature

The effects of the pressure and temperature on the ΔG profile for the carboxylation reactions (Scheme 3) of the two complexes (Ru with NNTs-□AA and PP) are computed in the gas phase at temperature 0, 25, and 100°C under pressures 1 and 10 atm. The Gibbs free energy values are greatly improved under 100 atm at room temperature (25 °C), as shown in SI (Table S7).

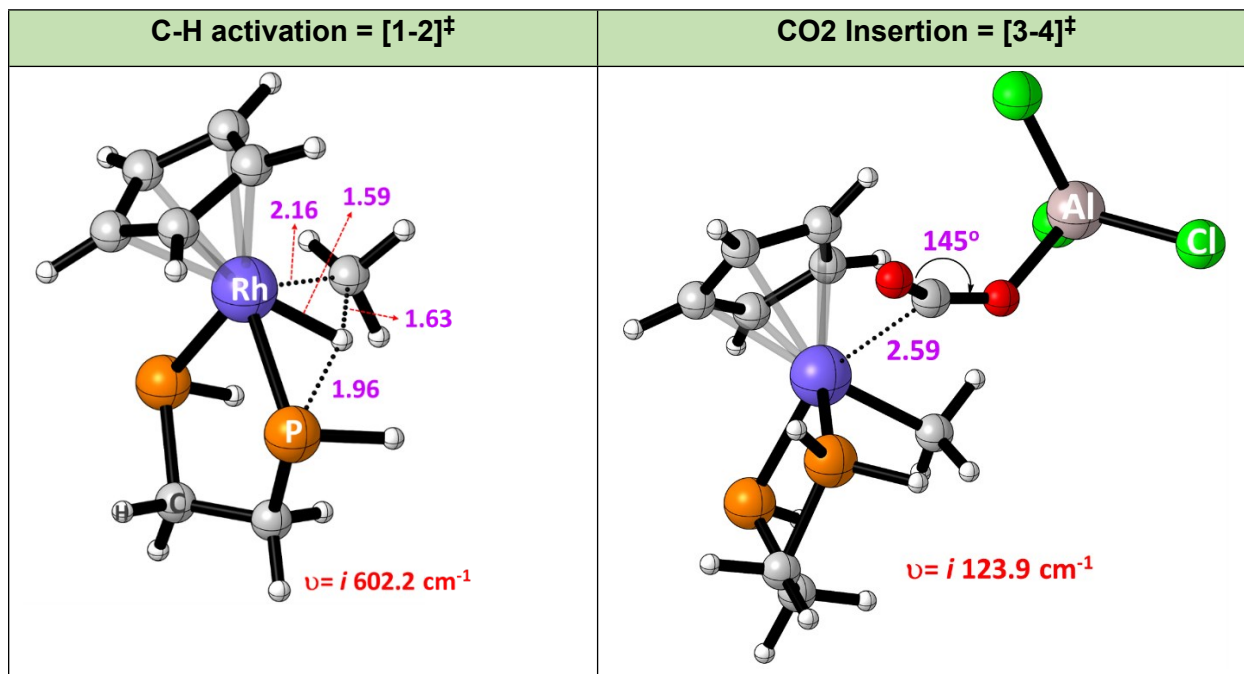
Table S7. The effects of the temperature and pressure of the relative ΔG for the formation of acetates using Ru with NNTs-□AA/PP complexes in the presence of AlCl₃, at the M06/(6-31G**,SDD) level.

P=atm T=°C	Ru-NNTs-□AA						Ru-PP				
	P=1, T=25	P=10, T=25	P=100, T=25	P=1, T=100	P=10, T=100	P=1, T=25	P=10, T=25	P=100, T=25	P=1, T=100	P=10, T=100	
1	5.5	4.2	2.8	8.2	6.4	8.0	6.6	5.2	10.5	8.8	
[1-2]‡	27.3	25.9	24.6	30.5	28.8	20.4	19.0	17.7	23.4	21.7	
2	9.1	7.7	6.4	12.1	10.4	19.3	18.0	16.6	22.3	20.6	
3	11.2	7.1	3.0	20.2	15.1	3.3	-0.8	-4.9	11.3	6.2	
[3-4]‡	23.3	19.2	16.4	32.5	27.3	8.4	4.3	0.2	17.1	11.9	
4	20.6	16.5	12.4	29.6	24.5	6.8	2.7	-1.4	15.5	10.4	
5	13.4	9.3	5.2	22.2	17.1	1.2	-2.9	-7.0	24.6	5.0	
[5-6]‡	17.2	13.1	9.0	26.2	21.0	9.8	5.7	1.6	18.9	13.8	
6	-33.2	-37.3	-41.4	-24.2	-29.3	-45.9	-50.0	-54.1	-37.2	-42.3	

9. Mechanism, Energy profile and Transition states using Rh/Ir-PP



Scheme S3. Detailed mechanism of Rh-PP(C_5H_5) and corresponding Gibbs free energy profile of the Rh-PP(C_5H_5) (shown in red lines) and comparison of Gibbs free energy profiles of Ru-PP(C_6H_6)/Rh-PP(C_5H_5)/Ir-PP(C_5H_5) complexes for the formation of CH_3COO^- from CH_4 and CO_2 in the presence of AlCl_3 at the M06/(6-31G**,SDD) level.



Reductive Elimination = [5-6][#]

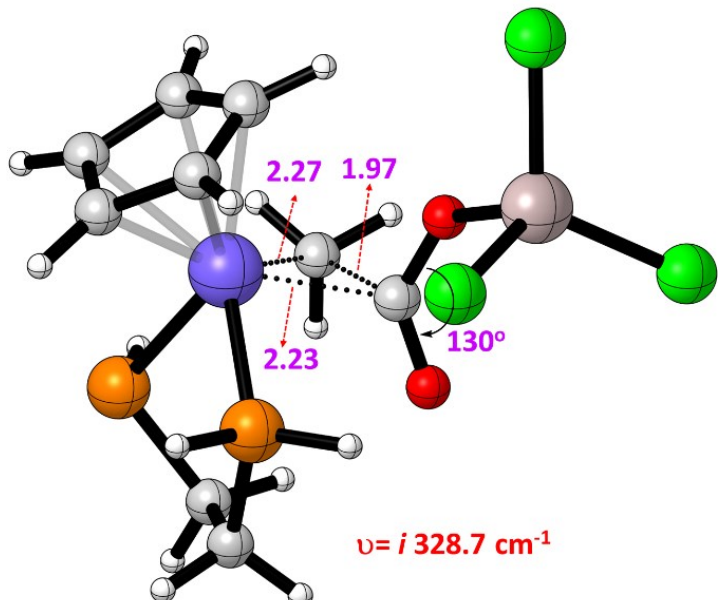


Figure S3. Optimized geometries of the transition states of Rh-PP complexes for the formation of CH₃COOH from CH₄ and CO₂ in the presence of Lewis acid (AlCl₃).

10. Effect in Gas vs Solvent Phase Optimization

The solvent optimization effects (benzene, toluene and dichloromethane (DCM)) are considered for the formation of carboxylation reactions of Scheme 3 and Scheme S2. The relative ΔG profiles are slightly deviated by 2-4 kcal/mol up and down from the gas phase energy profile. The details are shown in SI (Table S8).

Table S8. Relative Gibbs free energies (gas vs solvents optimization) for the formation of acetates using Ru with NNTs \square AA/PP metal ligand complexes in the presence of Lewis acids.

	Ru-NNTs.AA				Ru-PP			
	L1	L2	L3	L4	L1	L2	L3	L4
1	5.5	7.4	6.3	7.7	8.0	9.8	7.4	9.4
[1-2]‡	27.3	28.6	28.4	29.0	20.4	22.4	23.8	22.1
2	9.1	10.0	10.9	10.3	19.3	20.9	23.1	20.6
3	11.2	15.0	15.4	16.1	3.3	6.6	7.7	6.3
[3-4]‡	23.3	25.0	27.0	25.9	8.4	9.4	9.9	9.3
4	20.6	18.0	16.1	18.6	6.8	-3.5	-9.7	-3.8
5	13.4	12.8	13.6	13.3	1.2	-3.5	-7.2	-3.9
[5-6]‡	17.2	16.7	16.1	17.4	9.8	5.4	1.1	5.1
6	-33.2	-36.5	-36.9	-35.8	-45.9	-46.4	-48.6	-46.6

L1=M06/(6-31G**,SDD)

L2=SMD_(toluene)/M06/(6-31G**,SDD)

L3=SMD_(DCM)/M06/(6-31G**,SDD)

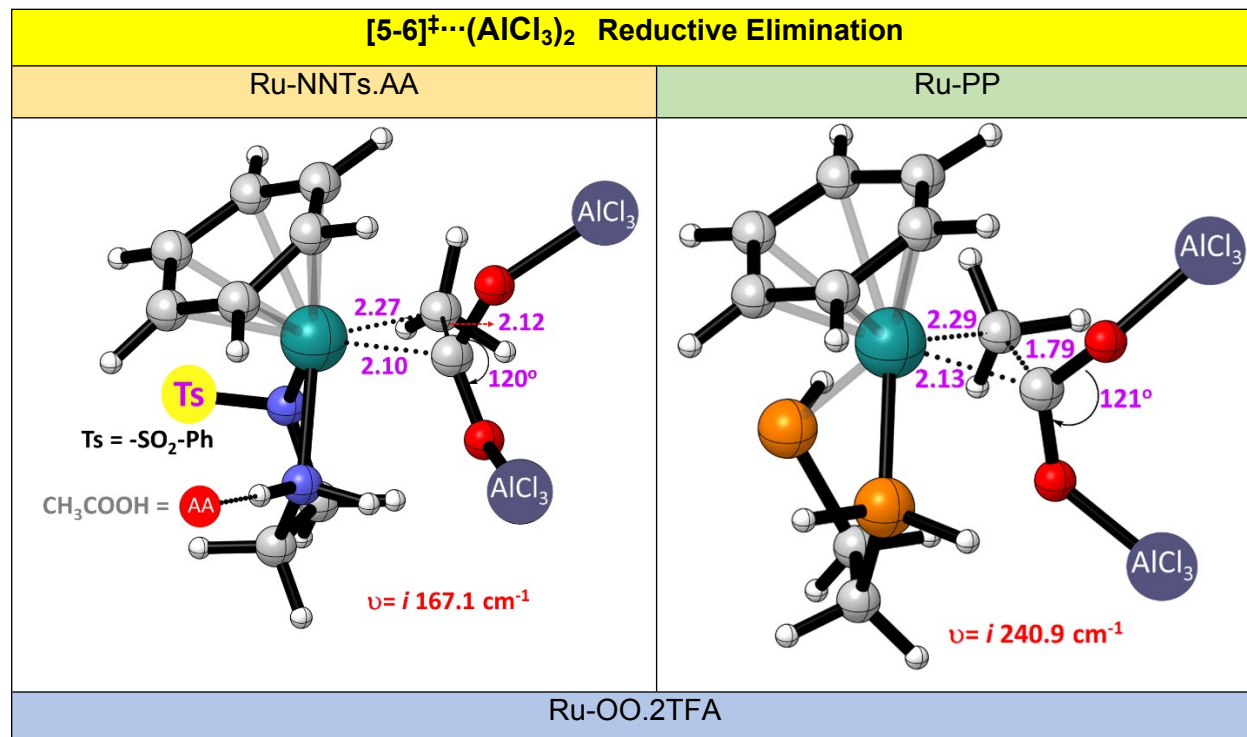
L4=SMD_(benzene)/M06/(6-31G**,SDD)

11. CO₂ activation using 2 molecules of AlCl₃

Table S9. Comparison of relative ΔG barriers (for separated reactants) for the elementary step of C-C bond formation between CH₃ and CO₂ ([5-6][‡]) using Ru-PP/NNTs-AA/OO-2TFA complexes in the presence of one or two AlCl₃ molecules at the M06/6-31G**,SDD level. Transition state models and their bond distances (Å) of Ru-NNTs-AA are given.

No. of molecules	(5)	[5-6] [‡]	(6)	Elementary step barrier	[5-6] [‡]
Ru-PP					
1.AlCl ₃	1.2	9.8	-45.9	8.6	
2.AlCl ₃	-24.7	-14.6	-63.6	10.1	
Ru-NNTs-AA					
1.AlCl ₃	13.4	17.2	-33.2	3.8	
2.AlCl ₃	-7.7	-2.4	-68.4	5.3	
Ru-OO.2TFA					
1.AlCl ₃	25.2	29.1	-22.9	3.9	
2.AlCl ₃	13.6	16.5	-40.2	2.9	

PRC=pre-reacting complex



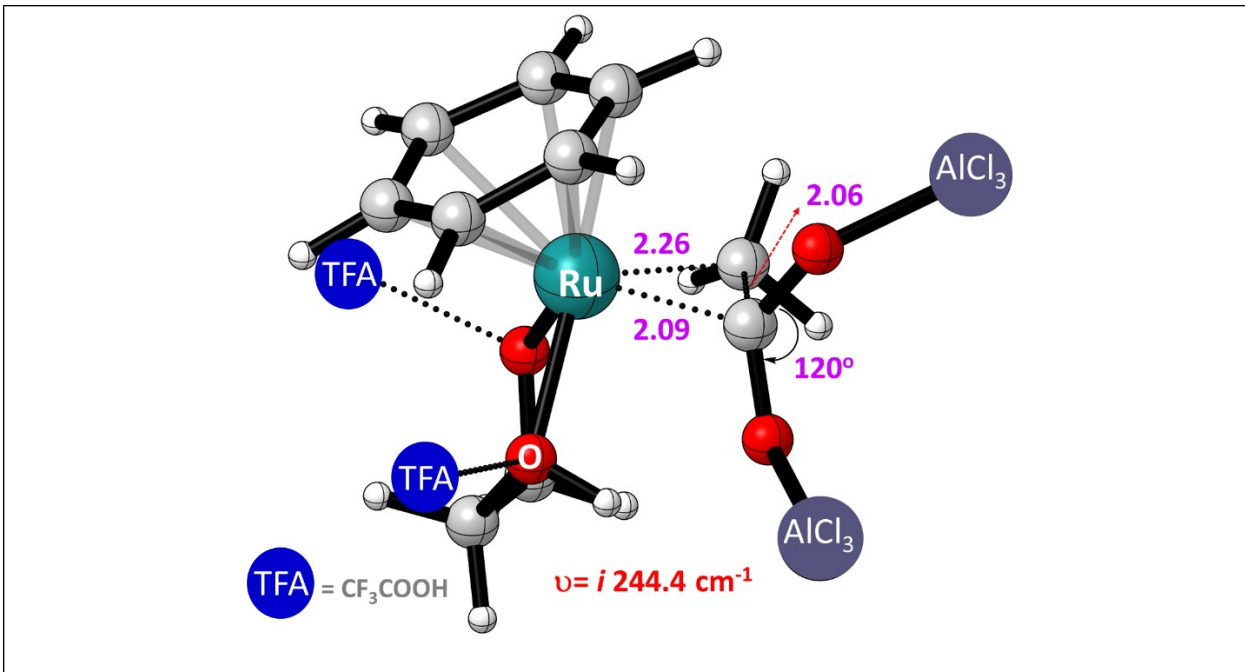


Figure S4. Optimized geometries of the transition states of C-C bond formation [5-6][‡] using Ru-PP/NNTs.AA/OO.2TFA complexes in the presence of two molecules of Lewis acid (AlCl_3)₂.

12. Effect of Basis sets and Quasi Approximation on Gibbs Free Energy Profiles

Effects of Quasi Approximation

Gibbs free energies (ΔG) are calculated by using the quasi-harmonic entropic approximation (QHA) based on the Grimme and Truhlar method (the frequency cut-off was 100 cm^{-1}).³⁰ However, we found that a half of QHA correction is more realistic, close to the experimental value for the $\text{CH}_4 + \text{CO}_2 = \text{CH}_3\text{COOH}$ reaction (see Table S1). Thus, to estimate the range of predicted values, we added 50% QHA corrected values (half of the difference in frequency cut-off 100 cm^{-1} value to the non-quasi) (see 50% quasi treatment of relative Gibbs free energy profiles in benzene solvent optimizations (Table S10)).

Table S10. Relative Gibbs free energies (gas, solvent, solvent+quasi) for the formation of acetates using Ru with NNTs \square AA/OO \square 2TFA/PP metal ligand complexes in the presence of Lewis acids.

	Ru-NNTs \square AA					Ru-OO \square 2TFA			Ru-PP				
	L1	L2 \square	L3 \square	L4	L4+ QHA/2	L1	L2 \square	L3 \square	L1	L2 \square	L3 \square	L4	L4+ QHA/2
1	5.5	6.2	6.6	7.7	4.8	5.0	5.8	6.4	8.0	8.1	8.6	9.4	6.8
[1-2]‡	27.3	28.9	30.6	29.0	26.3	28.6	27.4	28.6	20.4	22.7	23.4	22.1	19.5
2	9.1	11.1	14.0	10.3	7.8	20.5	18.8	21.9	19.3	21.6	22.1	20.6	18.0
3	11.2	15.4	18.8	16.1	8.8	29.2	28.5	33.4	3.3	6.8	9.0	6.3	-0.1
[3-4]‡	23.3	27.4	34.3	25.9	18.8	34.6	36.2	42.8	8.4	10.2	14.8	9.3	2.7
4	20.6	18.7	28.2	18.6	11.9	29.5	26.5	37.0	6.8	1.2	7.5	-3.8	-10.7
5	13.4	14.0	24.4	13.3	6.9	25.2	21.6	31.2	1.2	-6.2	0.9	-3.9	-10.7
[5-6]‡	17.2	17.5	27.7	17.4	10.8	29.1	25.4	34.7	9.8	2.8	9.9	5.1	-1.8
6	-33.2	-34.2	-26.0	-35.8	-42.3	-22.9	-24.2	-16.6	-45.9	-47.6	-40.8	-46.6	-53.3

L1: M06/(6-31G**,SDD)

L2 \square : [SMD_(DCM)/M06/(6-31G**,SDD)]//M06/(6-31G**,SDD)

L3 \square : [SMD_(DCM) /M06/6-311++G**,defTZVP]//M06/(6-31G**,SDD)

L4: SMD_(benzene)/M06/(6-31G**,SDD)

QHA/2: 50% quasi treatment.

13. Effects of Substitution on Ligands

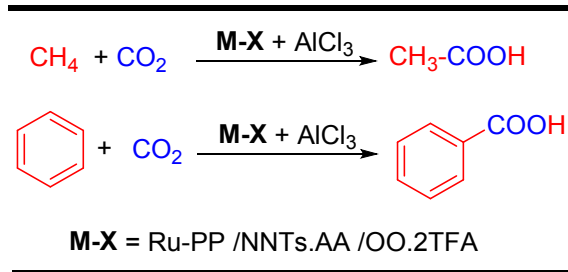
Calculations have been performed using simplified models of the ligands, in which phenyl substituents have been substituted by hydrogen atoms of carbons. We have computed one system with actual ligands using phenyl substituents (Noyori-Ikariya asymmetric ligands). The energy difference of real ligand and model ligand is minor (smaller than 1-2 kcal/mol) and more details are given in SI (Table S11).

Table S11. Relative Gibbs free energies for the formation of acetates (Scheme 3) using Ru metal with model vs real NNTs.AA ligand in the presence of Lewis acid (AlCl_3) at the M06/(6-31G^{**},SDD) level of theory.

	Model Ligand	Real Ligand
1	5.5	3.9
[1-2][‡]	27.3	30.9
2	9.1	12.9
3	11.2	9.9
[3-4][‡]	23.3	24.3
4	20.6	20.9
5	13.4	12.6
[5-6][‡]	17.2	15.9
6	-33.2	-40.1

14. Comparison of CO₂ Activations for sp³(CH₄) versus sp²(C₆H₆)

Our interest is also to test the catalytic activity of the sp³ vs sp² C-H activation using CH₄ and C₆H₆ molecules (Scheme S4). We also used the present successful metal-ligand complexes in the presence of co-catalysts (acids and Lewis acids) for the formation of CH₃-COOH and C₆H₅-COOH using CH₄ and C₆H₆ molecules, respectively, reacting with CO₂. We calculated ΔG of these two C-H activations and corresponding C-C bond formation steps in the presence of Lewis acid (Table S12). For sp³/sp² C-H activation, free energy barriers of benzene reacting with CO₂ are much lower than those of CH₄, at least by 4-8 kcal/mol in both C-H activation and CO₂ activation steps using Ru-PP/NNTs complexes.



Scheme S4. Comparison of sp³ vs sp² C-H activations of CH₄ vs benzene molecules.

Table S12. Relative Gibbs free energy barriers (from separated reactants) for the formation of CH₃COO⁻ and C₆H₅COO⁻ (Scheme S2 using Scheme 3) using Ru with PP/NNTs.AA/OO.2TFA in the presence of AlCl₃ at the M06/(6-31G**,SDD) level of theory.

	C-H activation	C-C bond formation
sp ³ vs sp ²	[1-2] [‡]	[5-6] [‡]
Ru-PP		
CH ₃ -COO ⁻	20.4	9.8
C ₆ H ₅ -COO ⁻	12.2	2.5
Ru-NNTs.AA		
CH ₃ -COO ⁻	27.3	17.2
C ₆ H ₅ -COO ⁻	24.7	9.9
Ru-OO.2TFA		
CH ₃ -COO ⁻	28.6	29.1
C ₆ H ₅ -COO ⁻	22.6	--

15. NBO Analysis of CH₄ and CO₂ activation steps

(i) CH₄ activation

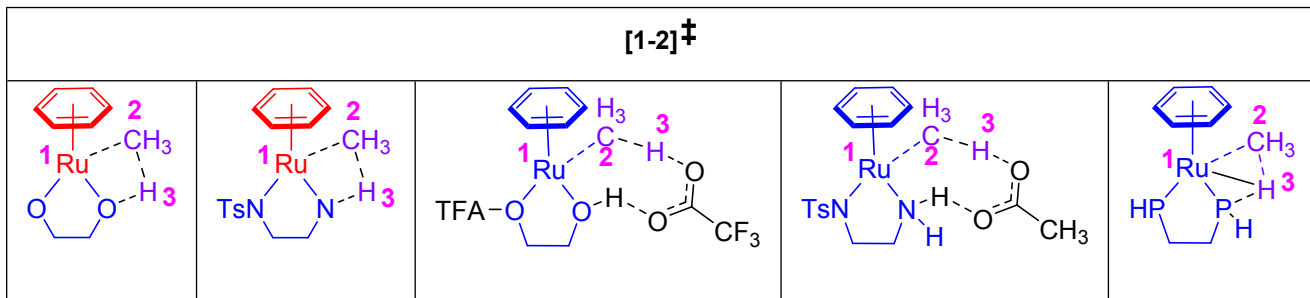


Figure S5. C-H activation transition state models using Ru-OO, Ru-OO.2TFA, Ru-NNTs, Ru-NNTs.AA and Ru-PP complexes

Table S13. NBO charges of Ru, C and H of C-H activation transition states using Ru-OO, Ru-OO.2TFA, Ru-NNTs, Ru-NNTs.AA and Ru-PP complexes. Gibbs free energy barriers of with and without additive (TFA/AA) have also given.

	$[1-2]^\ddagger$			
	Ru	C	H	ΔG^\ddagger
CH ₄		-0.95067	0.23767	
Ru-OO	0.11816	-1.02650	0.41868	34.7
Ru-OO.2TFA	0.09778	-1.05421	0.42263	28.6
Ru-NNTs	-0.03176	-0.99446	0.39048	40.2
Ru-NNTs.AA	-0.02005	-1.03809	0.41422	27.3
Ru-PP	-0.88634	-0.79464	0.22605	20.4

(ii) CO₂ activation

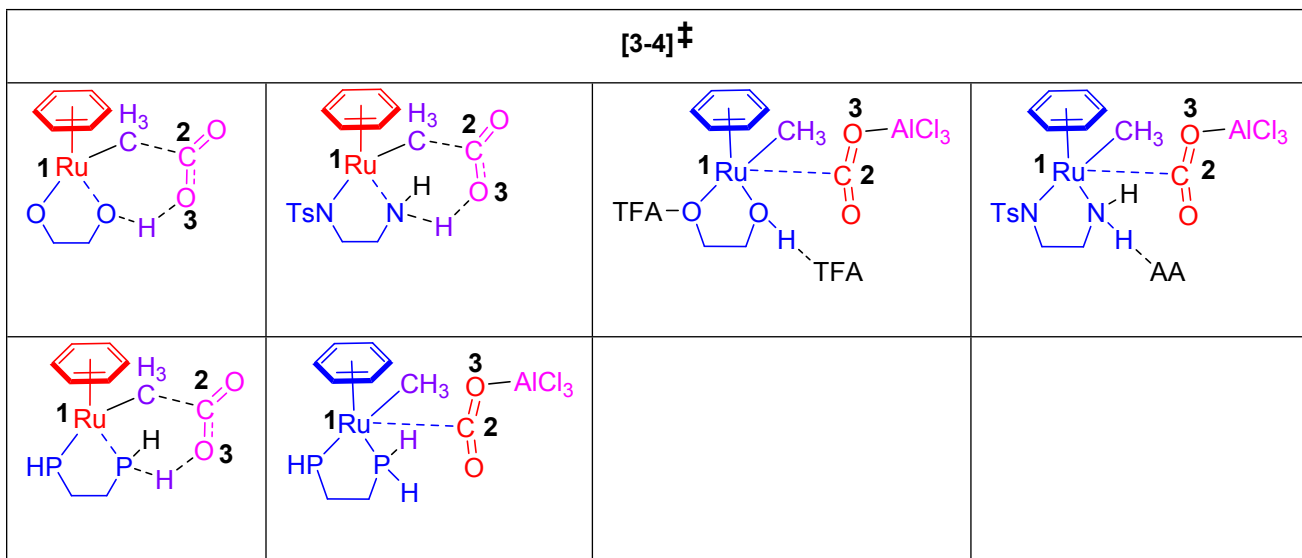


Figure S6. CO₂ activation transition state models using Ru-OO, Ru-OO.2TFA, Ru-NNTs, Ru-NNTs.AA and Ru-PP complexes and in the presence of Lewis acid AlCl₃ complex (CO₂ insertion TS step only given).

Table S14. NBO charges of Ru, C and O of CO₂ activation transition states using Ru-OO, Ru-OO.2TFA, Ru-NNTs, Ru-NNTs.AA and Ru-PP complexes and in the presence of Lewis acid AlCl₃ complex (CO₂ insertion TS step only given here). Gibbs free energy barriers of with and without additive (AlCl₃) have also given.

	$[3-4]\ddagger$			
	Ru-1	C-2	O-3	ΔG^\ddagger
CO ₂		1.08689	-0.54345	
Ru-OO	0.10096	0.97563	-0.63160	50.2
Ru-OO.2TFA-AlCl ₃	-0.02913	1.13179	-0.66960	34.6
Ru-NNTs	-0.02278	0.98094	-0.69611	48.3
Ru-NNTs.AA-AlCl ₃	-0.13851	1.08020	-0.72118	23.3
Ru-PP	-0.70649	0.93204	-0.69939	46.4
Ru-PP-AlCl ₃	-0.90162	1.06039	-0.72053	8.4

References

- [1] (a) Ribeiro, R. F.; Marenich, A. V.; Cramer, C. J.; Truhlar, D. G. *J. Phys. Chem. B* **2011**, *115*, 14556–14562; b) Grimme, S. *Chem. - Eur. J.* **2012**, *18*, 9955–9964; c) FunesArdoiz, I.; Paton, R. S. GoodVibes: GoodVibes v1.0.0 2016, 1. DOI 10.5281/zenodo.60811.
<https://zenodo.org/record/56091#.XgxVIczZPY>.
- [2] Wigner, E. *Phys. Rev.* **1932**, *40*, 749-759.
- [3] Bell, R. P. *Trans. Faraday Soc.* **1959**, *55*, 1-4.